Journal of Photochemistry and Photobiology A: Chemistry 220 (2011) 20–24

Contents lists available at ScienceDirect

Journal of Photochemistry and Photobiology A: Chemistry

journal homepage: www.elsevier.com/locate/jphotochem

Layer by layer TiO_2 thin films and photodegradation of Congo red

Maria T.C. Sansiviero[a,b,*], David S. dos Santos[b], Aldo E. Job[b,c], Ricardo F. Aroca[b]

[a] Departamento de Química, ICEx, Universidade Federal de Minas Gerais, Belo Horizonte, MG, Brazil
[b] Department of Chemistry and Biochemistry, University of Windsor, Windsor, Canada
[c] Faculdade de Ciência e Tecnologia, UNESP, Presidente Prudente, SP, Brazil

ARTICLE INFO

Article history:
Received 9 August 2010
Received in revised form 2 March 2011
Accepted 13 March 2011
Available online 21 March 2011

Keywords:
TiO_2
LbL film
Congo red
Photocatalysis
Resonance Raman scattering

ABSTRACT

Layer by layer (LbL) self-assembled technique was used to fabricate TiO_2 films onto glass and quartz slides. The LbL sequence was PAH/PSS/TiO_2(PSS/TiO_2)$_5$ (PSS = poly(sodium-4-styrene sulfonate), PAH = poly(allylamine hydrocloride)). These LbL thin films were characterized by Raman spectroscopy. The Raman spectrum confirmed the formation of TiO_2 nanoparticles in the anatase phase which average size of the particles around 30 nm and thickness of the film estimated around 40 nm as determined by atomic force microscopy (AFM). The photodegradation of Congo red (CR) dye immobilized over the LbL film was studied. Reference resonance Raman scattering (RRS) and Raman scattering (RS) spectra of Congo red were recorded with the 514.5 nm and 785 nm excitation laser lines. The photodegradation experiments were carried out by exposing the LbL TiO_2 film/CR to UV radiation in a container with distilled water. After UV exposure, degradation products were monitored by Raman spectroscopy.

1. Introduction

The layer by layer (LbL) self-assembly, is a established technique to form thin solid films onto a variety of substrates from solutions of materials with opposite charge [1,2]. Each exposure deposits a reproducible quantity of material and reverses the charge on the surface, leaving it primed for the next layer. These ultra-thin films may be assembled on a substrate by alternating exposure to solutions of different materials such as polyelectrolytes, proteins, dyes, metals, and nanoparticles among others [3,4]. Their structure and properties are strongly dependent on the chemical nature of interacting materials, the concentrations, and the physicochemical properties of the solutions, such as pH, ionic strength, and temperature. Since these polyelectrolyte multilayers present two-dimensionally stratified which are usually strongly interpenetrated, their behavior is dominated by internal interfaces, thus differing from the corresponding bulk material. Nanoparticles of TiO_2 has been immobilized in LbL films of PAH and poly(acrylic acid) (PAA), and used as photocatalyst for iodine oxidation and for decomposition of the dye methyl orange [5]. Titanium dioxide is a semiconductor with E_{gap} = 3.2 eV (388 nm), and it is widely used as a photocatalyst due to its high efficiency and low cost. TiO_2 occur in three known polymorphic forms such as anatase, rutile and brookite [6]. In general, the anatase form presents the better photocatalytic efficiency [7,8]. In environmental photocatalysis, TiO_2 is used to eliminate contaminants from textile wastes, and also to decompose pesticides and organochlorates [9]. Theoretical studies discuss the photoinduced electron transfer in dye-sensitized TiO_2 [10], an important approach for solar cells construction. The TiO_2 films continue to attract attention and there are very recent studies focusing on the production of TiO_2 patterns [11], for potential applications in selective adsorption of organic dye molecules in a mesoporous TiO_2 film [12].

This work aims to prepare and characterize LbL thin films of polymers/TiO_2 by Raman spectroscopy, which is a very accurate technique to identify the phases of TiO_2. In addition, the photodegradation of Congo red (CR) dye adsorbed over the TiO_2 LbL film was also investigated. The resonance Raman scattering (RRS) has been used to characterize the CR thin film, once that the electronic absorption of CR is in resonance with the laser line at 514.5 nm.

2. Experimental

The chemicals and solvents were supplied by Aldrich and Merck. TiO_2 nanoparticles were prepared from hydrolysis of titanium tetrabutoxide according to procedure from Ref. [4]. A solution of isopropanol (30 mL) and titanium tetrabutoxide (30 mL) was slowly added to 300 mL deionized water drop by drop under vigorous stirring. To this mixture 2.0 mL of a 70% nitric acid (pH 2.0) was added. The resulting solution was stirred for 2 h at room tempera-

* Corresponding author at: Departamento de Química, ICEx, Universidade Federal de Minas Gerais, Av. Antônio Carlos, 6627, CEP 31270-901, Belo Horizonte, MG, Brazil Tel.: +55 31 3409 5763; fax: +55 31 3409 5700.
E-mail address: mtcaruso@gmail.com (M.T.C. Sansiviero).

1010-6030/$ – see front matter © 2011 Elsevier B.V. All rights reserved.
doi:10.1016/j.jphotochem.2011.03.007

ture. The mixture was then heated to 80 °C while stirring for 4 h. The mixture solution was stirred overnight resulting in slightly cloudy TiO_2 solution. UV–visible absorption spectra were obtained using a Cary 50 UV–visible spectrometer. Atomic force microscopy (AFM) measurements were performed on a Digital Instruments NanoScope IV in noncontact tapping mode with a n+-silicon tip (NSC 14 model, Ultrasharp) operating at a resonant frequency of 256 kHz. All images were collected with high resolution (512 lines with 512 samples/line) at a scan rate of 0.5 Hz. The data were collected under ambient conditions, and each scan was duplicated to ensure that any features observed were reproducible. Raman scattering experiments were conducted by employing a micro-Raman Renishaw InVia system with laser excitation at 514.5 nm and 785 nm. All measurements were made in a backscattering geometry, using 50× microscope objective with a numerical aperture value of 0.75. The photodegradation experiments were carried out by the exposing the LbL TiO_2 film/CR to UV radiation in a container with distilled water illuminated by a low-pressure mercury lamp (output at 254 nm, 16 W) kept at 10 cm distant from the TiO_2 film/CR for 24 h. The irradiance of the light on the sample was 214 $\mu W\,cm^{-2}$.

3. Results and discussion

3.1. Fabrication of the LbL thin films containing TiO_2 nanostructures

Glasses and quartz slides were cleaned using a oxidizing solution of water (5 parts), NH_4OH (1 part) and H_2O_2 (30%) (1 part) and heating up to 85 °C for 10 min. The substrate was then washed 6 times with distilled water and finally heated in distilled water for 20 min at 80 °C. Poly(allylamine hydrochloride) (PAH, Mw = 70,000 g/mol) and poly(sodium-4-styrene sulfonate) (PSS, Mw = 70,000 g/mol) were purchased from Aldricht and used as received. Both polymers were dissolved in deionized water (1 g/L) and pH was adjusted to 2.0 by adding HCl. The LbL thin films were fabricated by the alternated immersion for 20 min of the substrate into PAH aqueous solution (pH 2.0) and then into the PSS (pH 2.0), follow by immersion into the colloidal solutions of TiO_2 (pH 2.0). After deposition of each layer, the substrate was rinsed with distilled water for 30 s. After the second layer, only PSS and TiO_2 were used, and this sequence was repeated five times. The film obtained is named PAH/PSS/TiO_2(PSS/TiO_2)$_5$. The deposition of TiO_2 nanoparticle layers was characterized by UV–visible absorption spectroscopy, using the TiO_2 band gap as reference. TiO_2 nanoparticles absorb below 380 nm down to the instrumental limit (200 nm). TiO_2 adsorption was monitored at 236 nm. The absorbance increased linearly with the number of the TiO_2 layers as observed generally for the layer–layer films containing inorganic particles [5]. UV–vis spectrum and a plot of absorbance at 236 nm versus number of layer are showed in Fig. 1.

The azo dye (CR) was immobilized on PAH/PSS/TiO_2(PSS/TiO_2)$_5$ by dipping the film on a 10^{-3} mol L^{-1} CR aqueous solution for 20 h and followed by rinsing with distillated water and air drying.

The morphological characterization started with nanoparticles in the colloidal solution of TiO_2 to be used in the fabrication of the LbL film. The solution was dilute 100 times and one drop was cast on a support and dried in air. Fig. 2A shows the AFM image and the particle diameter was *ca.* 4.3 nm. The height is also about 4.3 nm. Fig. 2B shows AFM images of PAH/PSS/TiO_2(PSS/TiO_2)$_5$ film, formation of aggregates is evident and the particle diameter is *ca.* 30 nm. Fig. 2C shows AFM images of PAH/PSS/TiO_2(PSS/TiO_2)$_5$ film thickness measurement (the film was scratched with a needle for this measurement) that was 33.5 nm.

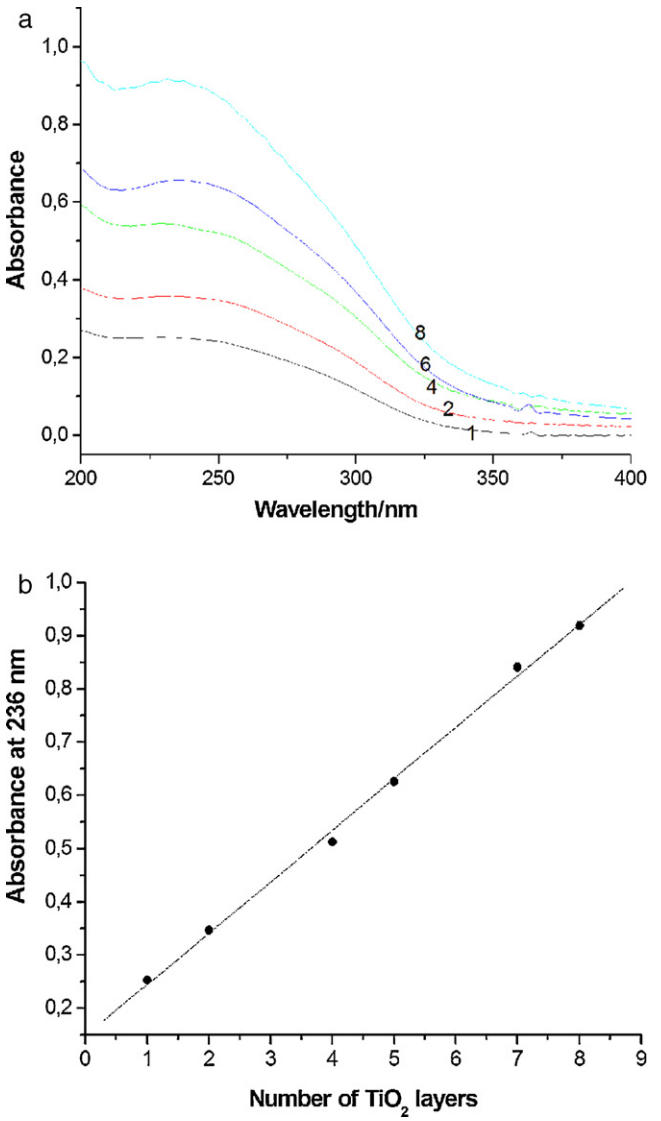

Fig. 1. UV–vis spectra of PAH/PSS/TiO_2(PSS/TiO_2)$_{n-1}$ thin films, where n is the number of TiO_2 nanoparticle layers, with n = 1, 2, 4, 6 and 8 (A) and absorbance at 236 nm versus number of TiO_2 layers (B).

3.2. Vibrational characterization and resonance Raman scattering

Fig. 3 shows the Raman spectra of PAH/PSS/TiO_2(PSS/TiO_2)$_5$ LbL film on a glass substrate and commercial anatase phase of TiO_2. Three strong peaks are observed in the LbL film that are assigned to TiO_2 anatase phase [6,13] at 637 cm^{-1}, 515 cm^{-1} and 405 cm^{-1}. These peaks are broadened and the 405 cm^{-1} band centre is slightly shifted with respect to those of a bulk crystal (bottom traces), that is observed at 395 cm^{-1}. The observed broadening line and shifting has also been shown in coupled CdS/TiO_2 systems [13], and it is attributed to the breakdown of the phonon momentum selection rule, specific of the Raman scattering in ordered systems. In the case of crystals of very small size, this rule is no longer valid as the phonons are confined in space and all the phonons over the Brillouin zone will contribute to the first order Raman spectra. The weight of the off-centre phonons increases as the crystal size decreases and the phonon dispersion causes an asymmetrical broadening and the shift of the Raman peaks [14].

The CR dye was immobilized over PAH/PSS/TiO_2(PSS/TiO_2)$_5$ film, by dipping the film on a 10^{-3} molar CR solution. Since CR in solution is negatively charged and TiO_2, the last layer, is positive,

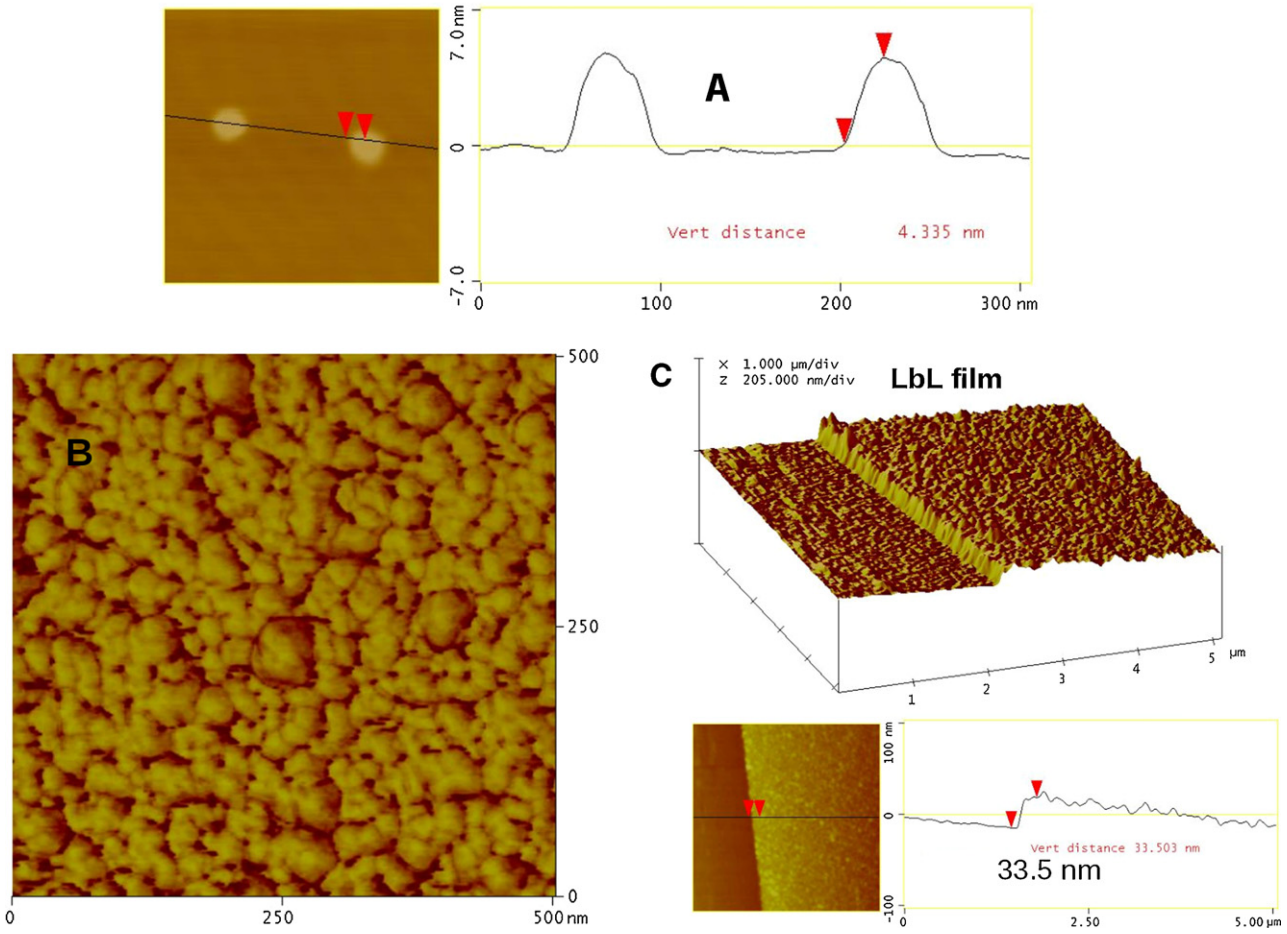

Fig. 2. AFM image of TiO_2 colloidal particles (A), AFM image of PAH/PSS/TiO_2(PSS/TiO_2)$_5$ thin film (B) and measurement of the film thickness (C).

the electrostatic attraction allows CR fixation over the TiO_2 film. The Raman scattering spectrum of CR obtained with the 785 nm laser line is presented in Fig. 4. The characteristic wavenumber of CR are seen in very narrow section of the full spectrum, and this section is shown in Fig. 4. The CR has an intense electronic absorption band at 498 nm and the excitation at 514.5 nm produces resonance Raman scattering (RRS). However, there is strong fluorescence background under 514.5 nm excitation. The fluorescence is quenched on metal surfaces, as it is done in surface enhanced resonance Raman scattering (SERRS) [15]. The SERRS spectrum of CR is given in Fig. 4. The SERRS of CR is simply the enhanced version of the RRS spectrum

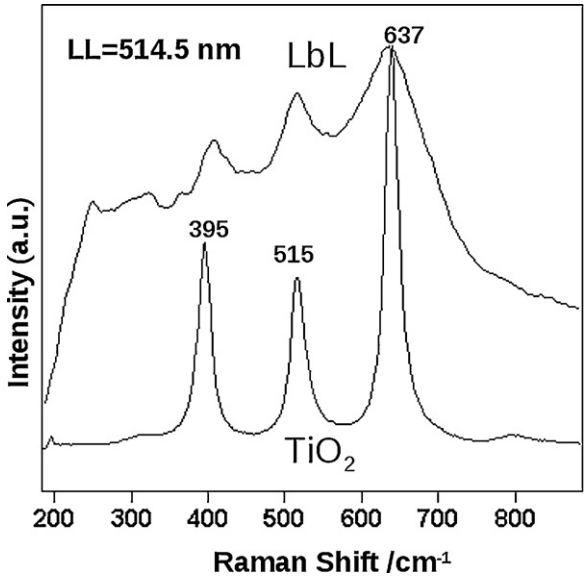

Fig. 3. Raman spectra of LbL PAH/PSS/TiO_2(PSS/TiO_2)$_5$ film and commercial anatase TiO_2.

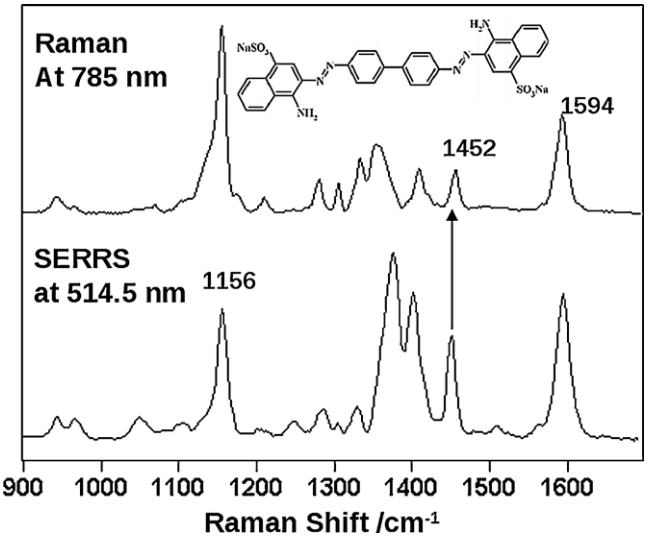

Fig. 4. Raman spectra of Congo red powder excited with the 785 nm laser line and SERRS of the CR on silver island film excited with the 514.5 nm laser line.

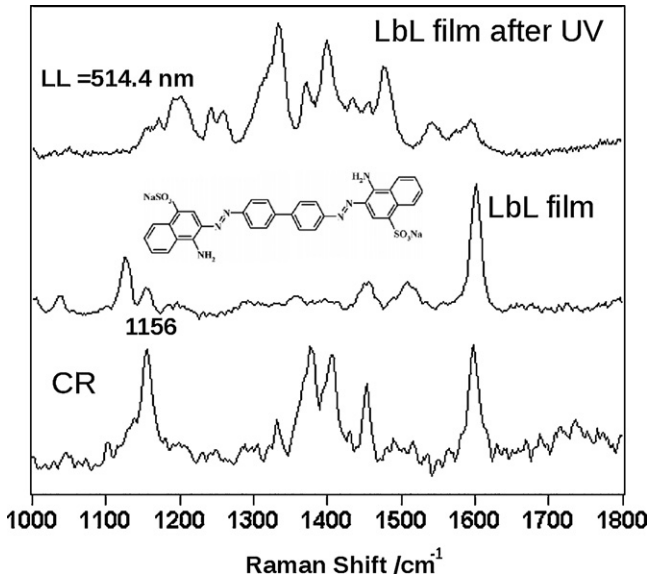

Fig. 5. Raman spectra of CR film UV irradiated (top), CR over PAH/PSS/TiO_2(PSS/TiO_2)$_5$ film (middle) and RRS of CR at 514.5 nm (bottom).

with minor variations in relative intensities. Most important is that this section of the complete spectrum can be used to characterize the CR, and has been used to follow the mechanism of binding of the marker dye Congo red in bio-medical applications [16].

PAH/PSS/TiO_2(PSS/TiO_2)$_5$/CR thin film was irradiated for 24 h using an Hg lamp. The Raman spectra of PAH/PSS/TiO_2(PSS/TiO_2)$_5$/CR film is shown in Fig. 5 before (middle traces) and after UV irradiation (top traces). The RRS spectrum of CR is also given as a reference. After irradiation several new Raman bands at 1578, 1541, 1476, 1333 (the most intense), 1206, 1191, 950 and 911 cm^{-1} appear. The bands observed at *ca.* 1206 and 1191 cm^{-1}, have been discussed by Corio and co-workers [17] as products detected in the spectrum of CR after electrochemical oxidation (+0.4 and +0.5 V). These observations point to the oxidation process of the CR.

In the direct photocatalysis, both positive holes and hydroxyl radicals have been proposed as the oxidizing species responsible for initiating the degradation of the organic substrates [18]. This mechanism is important when photocatalytic oxidation is conducted in the presence of water (as it was done on our experiment), the holes are efficiently scavenged by water and generate hydroxyl radicals $OH^{\bullet}$, which are strong and unselected oxidant species in favor of totally oxidative degradation for organic substrates. The process may be represented as follows:

$$TiO_2 + \text{UV light} \rightarrow e^-_{CB} + h^+_{VB} \quad (1)$$

$$h^+_{VB} + H_2O_{ads} \rightarrow OH_{ads}{}^{\bullet} + H^+ \quad (2)$$

$$h^+_{VB} + OH^- \rightarrow OH_{ads}{}^{\bullet} \quad (3)$$

$$e^-_{CB} + O_{2\,ads} \rightarrow O^-_{2\,ads} \quad (4)$$

The aromatic rings are exposed to successive attacks by photogenerated OH radicals, leading to hydroxylated metabolites before the ring opening. Thus, the most intense new band at 1333 cm^{-1} could be tentatively assigned to C–N stretching of semiquinone as was observed by Temperini and co-workers [19] on electrochemical oxidation of anilinium ions intercalated on montmorillonite clay. The band observed at 1191 cm^{-1} was tentatively assigned to C–H bending of benzenoid [19].

Characteristic Raman bands of CR (in SERRS and RRS) at, 1595 (phenyl ring), 1457 (N=N stretching), and 1155 cm^{-1} (N-phenyl), appear with very low intensity after irradiation (Fig. 5). A decrease in intensities could be assigned to process of photoisomerization of CR. He and co-workers [20] have observed that the photodegradation process occurs simultaneously with photoisomerization. They also observed that the relative intensity of some bands decreased during irradiation and they correlated the intensity change with trans ↔ cis photoisomerization of azobenzenes.

4. Conclusions

TiO_2 thin films were fabricated LbL electrostatic self-assembly method. The LbL TiO_2 thin film was characterized by Raman microscopy. The TiO_2 nanostructures (anatase phase) formed in the LbL film can be monitored in the Raman spectra thanks to the typical broadening of the Raman bands and small shift of the band centre. AFM images corroborated the inelastic scattering results and particle size of about 30 nm and film thickness of 33.5 nm was determined.

The CR immobilized on the film was subjected to photocatalysis. CR adsorption was achieved by the electrostatic attraction: TiO_2 layer is positively charged while CR in solution is negatively charged. Resonance Raman spectrum of CR dye immobilized over TiO_2 shows the characteristic CR modes at 1596 cm^{-1} (phenyl ring) and 1155 cm^{-1} (ϕ-N_{azo} stretching). After irradiation the film with a UV lamp, a very crowded Raman spectrum is recorded with several new bands, likely due oxidation process on CR molecule.

Acknowledgments

Financial assistance from the Natural Science and Engineering Research Council of Canada (NSERC) is gratefully acknowledged. Maria T.C. Sansiviero is gratefully to Conselho Nacional de Desenvolvimento Científico e Tecnológico (CNPq) for the fellowship at Department of Chemistry and Biochemistry University of Windsor.

References

[1] G. Decher, Fuzzy nanoassemblies: toward layered polymeric multicomposites, Science 277 (1997) 1232–1237.
[2] G. Decher, M. Eckle, J. Schmitt, B. Struth, Layer-by-layer assembled multicomposite films, Curr. Opin. Colloid Interface Sci. 3 (1998) 32–39.
[3] N.P.W. Pieczonka, P.J.G. Goulet, R.F. Aroca, Chemically selective sensing through layer-by-layer incorporation of biorecognition into thin film substrates for surface-enhanced resonance Raman scattering, J. Am. Chem. Soc. 128 (2006) 12626–12627.
[4] F. Huguenin, V. Zucolotto, A.J.F. Carvalho, E.R. Gonzalez, O.N. Oliveira, Layer-by-layer hybrid films incorporating WO_3, TiO_2, and chitosan, Chem. Mater. 17 (2005) 6739–6745.
[5] T.H. Kim, B.H. Sohn, Photocatalytic thin films containing TiO_2 nanoparticles by the layer-by-layer self-assembling method, Appl. Surf. Sci. 201 (2002) 109–114.
[6] M. Ben Yahia, F. Lemoigno, T. Beuvier, J.-S. Filhol, M. Richard-Plouet, L. Brohan, M.-L. Doublet, Updated references for the structural, electronic, and vibrational properties of TiO2(B) bulk using first-principles density functional theory calculations, J. Chem. Phys. 130 (20) (2009), 204501/1–204501/11.
[7] A.L. Linsebigler, G.Q. Lu, J.T. Yates, Photocatalysis on TiO_2 surfaces – principles, mechanisms, and selected results, Chem. Rev. 95 (1995) 735–758.
[8] A. Sclafani, M.N. Mozzanega, P. Pichat, Effect of silver deposits on the photocatalytic activity of titanium-dioxide samples for the dehydrogenation or oxidation of 2-propanol, J. Photochem. Photobiol. A 59 (1991) 181–189.
[9] M.R. Hoffmann, S.T. Martin, W.Y. Choi, D.W. Bahnemann, Environmental applications of semiconductor photocatalysis, Chem. Rev. 95 (1995) 69–96.
[10] W.R. Duncan, O.V. Prezhdo, Theoretical studies of photoinduced electron transfer in dye-sensitized TiO_2, Annu. Rev. Phys. Chem. 58 (2007) 143–184.
[11] G. Shi, N. Lu, L. Gao, H. Xu, B. Yang, Y. Li, Y. Wu, L. Chi, Fabrication of TiO_2 arrays using solvent-assisted soft lithography, Langmuir 25 (2009) 9639–9643.
[12] K. Lee, S. Park, M.J. Ko, K. Kim, N.-G. Park, Selective positioning of organic dyes in a mesoporous inorganic oxide film, Nat. Mater. 8 (2009) 665–671.
[13] J.C. Tristão, F. Magalhães, P. Corio, M.T.C. Sansiviero, Electronic characterization and photocatalytic properties of CdS/TiO_2 semiconductor composite, J. Photochem. Photobiol. A 181 (2006) 152–157.
[14] D. Bersani, P.P. Lottici, X.-Z. Ding, Phonon confinement effects in Raman scattering by TiO_2 nanocrystals, Appl. Phys. Lett. 72 (1998) 73–75.
[15] R.F. Aroca, Surface-enhanced Vibrational Spectroscopy, 1st ed., John Wiley & Sons, Chichester, 2006.
[16] J. Sajid, A. Elhaddaoui, S. Turrell, Investigation of the binding of Congo red to amyloid in Alzheimer's diseased tissue, J. Mol. Struct. 408/409 (1997) 181–184.

[17] C.E. Bonancêa, G.M. Nascimento, M.L. Souza, M.L.A. Temperini, P. Corio, Substrate development for surface-enhanced Raman study of photocatalytic degradation processes: Congo red over silver modified titanium dioxide films, Appl. Catal. B 69 (2006) 34–42.
[18] J.T. Yates Jr., Photochemistry on TiO_2: mechanisms behind the surface chemistry, Surf. Sci. 603 (2009) 1605–1612.
[19] G.M. Nascimento, A.C.M. Padilha, V.R.L. Constantino, M.L.A. Temperini, Oxidation of anilinium ions intercalated in montmorillonite clay by electrochemical route, Colloid Surf. A: Physicochem. Eng. Aspects 318 (2008) 245–253.
[20] J.-A. He, S. Bian, L. Li, Jayant Kumar, S.K. Tripathy, A.L. Samuelson, Photochemical behavior formation of surface relief grating on self-assembled polyion/dye composite film, J. Phys. Chem. B 104 (2000) 10513–10521.